RESEARCH

A systematic regulatory network related to bulbil formation in *Lilium lancifolium* based on metabolome and transcriptome analyses

Ruiyi Ma[1], Yan Zhang[1], Jun Zhao[1], Yang Zheng[1], Li Xue[1*] and Jiajun Lei[1*]

Abstract

Background *Lilium lancifolium* is a special wild triploid species native to China and can produce abundant bulbils on its stem under natural conditions, which is very valuable to study bulbil organogenesis in plants. Although similar to the lateral and tillering principles, the molecular mechanism underlying bulbil formation has remained incompletely understood.

Results The metabolome and transcriptome of *L. lancifolium* bulbils across four development stages were analyzed. The pairwise comparison of metabolomes across the four stages identified 17 differential hormones, predominantly auxin (IAA), cytokinin (CK), and jasmonic acid (JA). Short Time-series Expression Miner (STEM) trend analysis of differential genes revealed four significant trends across these stages. The KEGG enrichment analysis of the four clusters highlighted pathways, such as plant hormone signal transduction, which were speculated to play a crucial role in development stages. these pathways were speculated to play a crucial role in development stages. To explore the key differential expressed genes and transcription factors associated with bulbil occurrence, two periods were focused on: LI_UN and LI_DN, which represented the stages with and without bulbils, respectively. Through correlation analysis and qRT-PCR analysis, 11 candidate differentially expressed genes and 27 candidate transcription factors were selected. By spraying exogenous hormones to validate these candidates, *LlbHLH128*, *LlTIFY10A*, *LlbHLH93*, and *LlMYB108*, were identified as the key genes for *L. lancifolium* bulbils.

Conclusion A regulatory network of *L. lancifolium* bulbil development was predicted. *LlTIFY10A* and *LlbHLH93* might be involved in the JA and auxin signal transduction pathways, which jointly formed a regulatory network to affect the occurrence of *L. lancifolium* bulbil. This study not only provided more information about the differentially expressed genes and metabolites through transcriptome and metabolomics analyses, but also provided a clearer understanding of the effect of hormones on bulbil formation in lily.

Keywords *Lilium lancifolium*, Bulbil formation, Transcriptome, Hormone, Transcription factors

*Correspondence:
Li Xue
lixue@syau.edu.cn
Jiajun Lei
jiajunlei@syau.edu.cn
[1]College of Horticulture, Shenyang Agricultural University,
Shenyang 110866, China

Ma *et al. BMC Plant Biology*   (2024) 24:969

Page 2 of 17

Introduction

The phenomenon of bulbil/bublet formation, observed in various plants such as *Polygonum viviparum*, *Sedum bulbiferum*, and *Laportea bulbifera*, serves as a significant reproductive organ to avoid certain issues associated with sexual reproduction, minimizing variation and enhancing reproductive efficiency [1]. *Lilium lancifolium*, commonly known as tiger lily, is a special wild triploid species and naturally distributes across 17 provinces in China. When mature bulbils detach from parent plants, they can develop into new plantlets, just like the seed's germination. In the genus *Lilium*, under natural condition only four species including *L. lancifolium*, *L. sulphureum*, *L. sargentiae*, and *L. bulbiferum* can form bulbils in leaf axils of the stem. But nowadays, propagation of lily cultivars in production primarily relies on bulb division. Inducing bulbil development can effectively enhance their reproductive efficiency. Nevertheless, there was few reports on the exploitation of bulbils as propagation materials in lily production. Although several studies on lily bulbil have been reported, they focused mainly on morphological observation and physiological index determination [2, 3]. The lily bulbils can originate from the leaf axillary meristem referred to as the lateral meristem [4, 5]. Fan et al.. emphasized that the cell growth within bulbils facilitated the rapid transport and accumulation of sucrose and other substances [3]. Moreover, several studies have indicated that bulbils can be induced by hormone treatments on the stem of lilies without bulbils, suggesting the complexity of bulbil occurrence. The transcriptome sequencing analysis of *L. lancifolium* bulbils has been carried out, and revealed the significance of starch and glycometabolism alongside the plant hormone signal transduction pathway in bulbil formation [2]. The regulatory role of auxin in bulbil development was confirmed, which was consistent with the findings of Luo et al. [6]. In addition to auxin, cytokinin can exhibit distinct regulatory roles in bulbil formation. During the bulbil initiation, the expression of *IPT1/5* and *LOG1/3/5/7* increased while *CKX4* decreased, subsequently elevating endogenous cytokinin levels and activated the cytokinin signaling pathway to regulate bulbil formation [7, 8]. In addition, the genes *WOX9* and *WOX11* in the *WOX* gene family may also regulate the bulbil occurrence, which reveals the molecular regulation mechanism of bulbil formation underlying the *WOX* gene and cytokinin signaling pathway [9].

The morphological and anatomical observations have revealed the similarities between the bulbils in lily and lateral branches in *Arabidopsis* and tillering in rice [1, 3, 5]. Extensive researches on the axillary branches showed that hormones have played the crucial role. Plant hormones such as IAA, CK, and GA regulate the formation and development of axillary meristem (AM) [10].

The IAA and ABA can partially inhibit axillary buds [11], with the low IAA level in leaf axils enhancing the AM formation, whereas high IAA concentration inhibiting axillary buds. Conversely, CK stimulate axillary bud growth [12, 13]. Moreover, GA and JA also serve as key regulators of various aspects of plant growth and development [14, 15]. Furthermore, there is a wide cross-reactivity among different phytohormone anabolic pathways, and the interaction is evident in the regulation of AM formation and development. Auxin can inhibit the AM growth by modulating cytokinin concentration [11]. The CK application at the axillary bud can promote the auxin accumulation, subsequently induce branching [16]. Additionally, IAA can induce changes in plant branches via JA [17]. The various hormones affect branching individually or interactively, and contribute to a complex regulatory network.

With the rapid advancement of omics technology, several related genes have been identified. Based on the transcriptome of *Ornithogalum arabicum*, Jiang et al. [18–21]. suggested significant changes in the expression of genes, such as *WOX8*, *KN1*, and *DCAF8*, suggesting their involvement in bulbil occurrence. The *MADS* and *KNOM* genes that have been extensively studied in *Agave* can play key roles in axillary bud development. For instance, the *MADS1* regulates axillary bud development in potato by modulating cell growth in the vegetative meristem [22]. The *KNOM* gene can regulate the cellular uncertainty in the meristem zone through the interactions with cytokinin and gibberellin [23], closely associated with the bulbil development [24, 25]. Liu et al. identified significant differential expression of *PEBP* gene families, including the *FT*, *TFL*, and *MFT* subfamilies, during bulblet formation in *Pinellia cordata*. These genes are known to regulate processes, such as tuber and bulb formation [26]. These findings have indicated that the multi-omics joint analysis is an effective strategy for identifying the key genes regulating these traits. This study systematically observed the development of bulbils in *L. lancifolium* and conducted the transcriptome and metabolome sequencing during the critical periods of bulbil development. This study aimed to screen for new regulatory mechanism through a multi-omics approach with the intention of identifying key genes for *L. lancifolium* bulbil initiation, and explore the regulatory network affecting this process. Additionally, this study could provide insights into the initiation and formation of *L. lancifolium* bulbils, as well as a foundation for future molecular researches on bulbil formation in *Lilium*.

Results

Overall hormonal situation changes and key hormonal analysis during bulbil development

Throughout the bulbil development, notable changes were observed in the hormone content. The PCA diagram indicated the clear clustering of three replicates, demonstrating significant differences between Ll_DN on the lower axil and the other stages (Ll_UN, Ll_UT, and Ll_UE) on the upper axil of the stem (Fig. S1A). A total of 41 hormones were identified, including auxin (IAA), cytokinin (CK), abscisic acid (ABA), jasmonic acid (JA), salicylic acid (SA), gibberellin (GA), and ethylene (ETH), with CKs comprising the highest proportion of components, followed by IAA and JAs. Additionally, distinct hormone profiles were observed during Ll_DN, Ll_UN, Ll_UT, and Ll_UE stages. The analysis of hormone accumulation revealed high levels of salicylic acid and auxin at Ll_DN stage, accounting for 97% of the total hormone content, which may explain the absence of bulbils in the lower part of the plant (Fig. 1E). Moreover, the total content of JA gradually increased, and the total content of IAA gradually decreased upon the occurrence of *L. lancifolium* bulbils (i.e., Ll_UN, Ll_UT). This suggested that both hormones played pivotal roles in inducing the bulbil development of *L. lancifolium*.

To precisely identify the key phytohormones influencing the bulbil development, a clustering heatmap was generated to visualize variations across different stages (Fig. 1F). The heatmap primarily revealed the variations in hormone types between the lower and upper axils, possibly linked to the presence of *L. lancifolium* bulbils. Some hormones were only detected in Ll_DN, such as IAA-Glc (1-O-indol-3-ylacetylglucose), IP (N6-isopentenyladenine), mTR (meta-Topolin riboside), cZROG (cis-Zeatin-O-glucoside riboside), DHZROG (Dihydrozeatin-O-glucoside riboside), BAP (6-Benzyladenine), and GA_{15} (Gibberellin A_{15}). Correspondingly, some hormones were only detected in the three stages on the upper axil (Ll_UN, Ll_UT and Ll_UE), such as TRA (Tryptamine), pTR (para-Topolin riboside), KR (Kinetin riboside), iP9G (Kinetin riboside), K9G (Kinetin-9-glucoside), and OPC-4 (3-oxo-2-(2-(Z)-Pentenyl). Among the hormones detected in all four stages, notable differences were observed between Ll_DN stage on the lower axil and the three stages on the upper axil, such as OPDA (cis(+)-12-Oxophytodienoic acid), JA, ABA, IAA, GA_1 (Gibberellin A_1), GA_3 (Gibberellin A_3), ACC (1-Aminocyclopropanecarboxylic acid), and SA. Most of these differential hormones exhibited their highest levels in Ll_DN stage, indicating their potential association with the absence of bulbils at this stage. Among them, SAG (salicylic acid 2-O-β-glucoside) showed the highest content (4953 ng/g), followed by TRP (L-tryptophan) (1724 ng/g).

The changes in hormone levels may be the primary factor contributing to the bulbil formation of *L. lancifolium*.

The comparative analysis of the hormone types in the samples was conducted to explore the predominant hormones influencing bulbil occurrence (Table S1). The table illustrates that the disparity in hormone metabolism between Ll_DN and Ll_UE was more pronounced, whereas Ll_UT vs. Ll_UE exhibited fewer differences. The differential hormones identified from the pairwise comparison were further refined through the relative quantification, and 17 differential hormones were finally selected. A correlation network diagram was generated to examine the relationship among the 17 identified differential hormones ($|rho| > 0.95$), which included ABA, cZROG, DHZROG, GA_3, IAA-Glc, IP, JA, JA-ILE (Jasmonoyl-L-isoleucine), JA-Val (N-[(-)-Jasmonoyl]-(L)-valine), MEJA (Methyl jasmonate), mTR (meta-Topolin riboside), OPC-4 (3-oxo-2-(2-(Z)-Pentenyl) cyclopentane-1-butyric acid, OPDA, SA, SAG, TRA, and TRP. Most of these hormones were positively correlated. Notably, no significant correlation was observed between the five JAs and other hormones, indicating their independence from the processes influencing bulbil occurrence and their lack of interaction with other hormone types. Negative correlations were only observed in ABA and TRA with other nine differential hormones, except for SA (Fig. 1G).

Global transcript analysis during bulbil development

The high-throughput sequencing of the samples was conducted using the Illumina Novaseq™ 6000 system, and 12 sequencing libraries were constructed from four samples representing different stages of bulbil development in *L. lancifolium*. All the raw reads were deposited in the NCBI Sequence Reads Archive (SRA) under accession number SRP505108. Following the removal of sequencing adapters and low-quality reads, the effective read counts for the four samples were 4.59×10^7, 5.26×10^7, 4.31×10^7, and 4.64×10^7, respectively. The statistical analysis revealed that the percentage of bases Q20 and Q30 in each sample exceeded 97.9% and 93.6%, respectively. Additionally, the GC content was consistent across the samples, averaging approximately 51% (Table S2). The trinity assembly yielded 107,265 transcripts, averaging 485 bp in length, with an N50 of 1,163 bp (Table S3). The results indicated that the data quality from the transcriptome sequencing satisfied the requirements for the database establishment, and that the assembly quality was suitable for subsequent analysis.

To verify the data reliability, the Pearson correlation analysis was conducted between the samples, as shown in Fig. S1B. The correlation between the three replicates within each group exceeded 0.9, indicating strong consistency and high reliability. Additionally, distinct
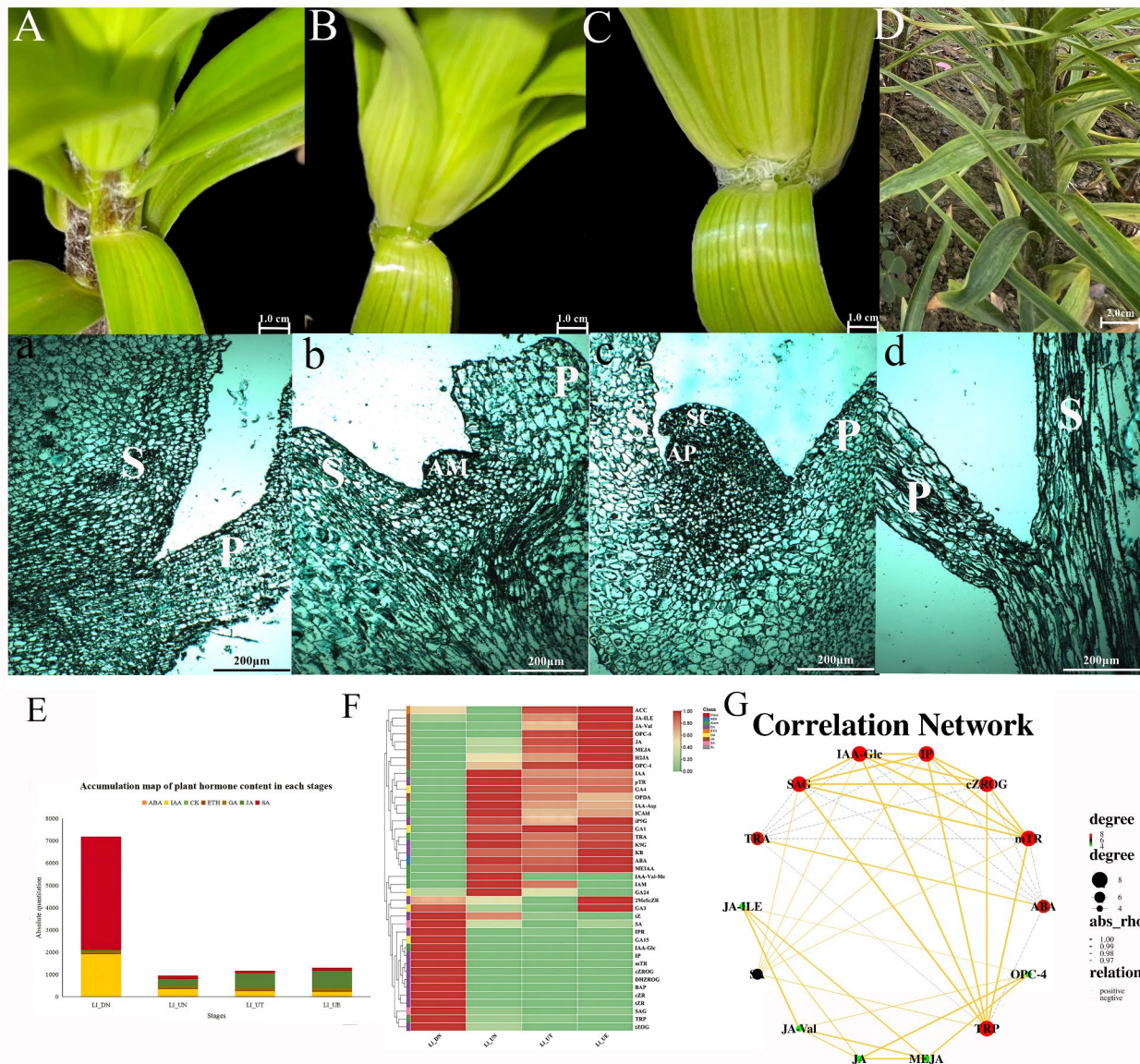
Fig. 1 Paraffin observation and global hormone analysis. (**A-D**) Different development stages of *Lilium lancifolium* bulbil. (a-d) Four stages of bulbil on the stem were observed using the paraffin section for transcriptome sequencing and metabolome determination: Ll_UN (no upper bulbils), Ll_UT (transparent bulges in upper leaf axils), Ll_UE (white bulges emerging in upper leaf axils), and Ll_DN (no bulbils at 10 cm down from the bottom). **P**: petiole; **S**: stem; **AP**: apical point; **SC**: scale; **AM**: axillary meristem. (**E-G**) Overall hormonal situation quality control during the different stages of *L. lancifolium* bulbil. (**E**) Dynamic changes of each hormone content during different stages. (**F**) Heat map of the differential metabolites. (**G**) Correlation between 17 differential hormones. Correlation coefficient |rho| ≥ 0.95

differences were observed between Ll_DN stage on the lower axil and the three stages (Ll_UN, Ll_UT, and Ll_UE) on the upper axil, which was consistent with the hormone analysis results. A total of 39,441 genes exhibited the co-expression across all four stages, with 1,450 genes exclusively co-expressed in the three stages of the upper axil and 384 genes specifically expressed in Ll_DN (Fig. 2A).

Among the 39,441 genes expressed across the four stages, 433 were transcription factors (Table S4), including 77 from the *bHLH* gene family, 51 from the *ERF* gene family, 17 from the *GATA* gene family, 83 from the *MYB* gene family, 47 from the *WRKY* gene family. There were 1,011 hormone-related genes. There are 347 genes annotated to the signal transduction pathway in KEGG, most of them annotated to the auxin signal transduction pathway, jasmonate signal transduction pathway,
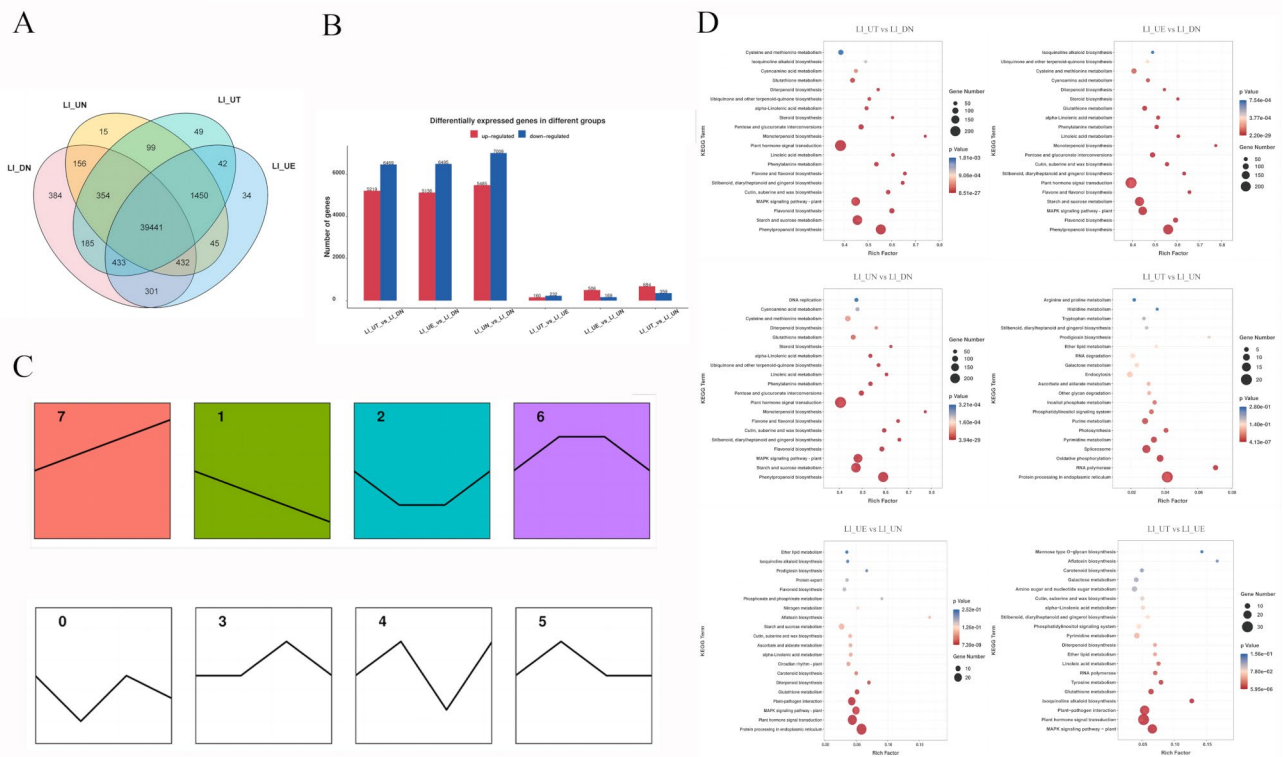
Fig. 2 Analysis of the genes in different stage of *L. lancifolium* bulbil. (**A**) Venn diagram. (**B**) Bar graph of the differential genes. (**C**) Differential gene trend analysis. (**D**) KEGG enrichment analysis for differential genes

brassinosteroid signal transduction pathway and gibberellin signal transduction pathway, and the remaining genes are distributed in different phytohormone synthesis and transduction pathways (Table S5).

Analysis of differentially expressed genes (DEGs) in different development stages of *L. lancifolium* bulbils

Differences between genes were selected through screening for fold differences equal to or greater than 2 (log2 fold-change value) and *P*-values or q-values less than 0.05. There was a greater number of differential genes between Ll_DN stage on the lower axil and the three stages (Ll_UN, Ll_UT, and Ll_UE) on the upper axil, as shown more distinctly in the histogram (Fig. 2B). Conversely, fewer differential genes were evident among the three stages on the upper axils. Specifically, 12,494 DEGs were identified between Ll_UN and Ll_DN, comprising 5,485 up-regulated and 7,009 down-regulated DEGs. Subsequently, Ll_UT vs. Ll_DN and Ll_UE vs. Ll_DN revealed 11,833 and 11,631 differential genes, respectively. In the pairwise contrast group of the three stages on the upper axil, Ll_UT vs. Ll_UN exhibited the highest number of differentially expressed genes, featuring 684 up-regulated and 359 down-regulated genes. Conversely, the contrast group Ll_UT vs. Ll_UE demonstrated the fewest differential genes, comprising 160 up-regulated

and 232 down-regulated genes. The KEGG analysis was conducted for the differential genes in these comparison groups, revealing significant enrichment in both plant hormone signal transduction and protein processing in the endoplasmic reticulum (ER). This enrichment indicated the likely involvement of hormones in the growth of *L. lancifolium* bulbils (Fig. 2D).

We combined the 23,193 differential genes from the pairwise comparisons to identify the differential genes for each of the four stages, which comprised 719 TFs and 582 hormone-related genes. To further identify key differential genes, we conducted STEM trend analysis on the high-quality data after removing low-quality samples, revealing four significant trends. To further investigate the main differential genes, the STEM trend analysis of the differential genes across the four stages after removing the low-quality data revealed four significant trends (Fig. 2C). Trend 7 exhibited a consistent up-regulation, while Trend 1 displayed a completely opposite pattern, featuring the continuous down-regulation. The genes under Trend 2 demonstrated a uniform increase across the three upper stages, whereas those under Trend 6 exhibited a collective decrease in the three upper stages. Owing to variations in *P*-values and gene lengths, the number of differential genes in Trends 7 and 1 exceeded 6,000, and the number of differential genes under Trends

Ma *et al. BMC Plant Biology*   (2024) 24:969

Page 6 of 17

2 and 6 was approximately 2,000. To gain a more intuitive understanding of the main pathways enriched by the differential genes across the four significant trends, the KEGG enrichment analysis was conducted for each cluster (Fig. S2A-D) individually. The results were to some extent consistent with the previous findings of differential gene enrichment. The most prominent enrichments included plant hormone signal transduction, ribosome, protein processing pathway in the endoplasmic reticulum, and MAPK signaling pathway. These pathways were speculated to be of significant importance during the developmental stages.

The correlation network diagrams were generated to further examine the relationship between the TFs and hormone-related genes for each trend (Fig. S3 A-D). A total of 112 TFs and 130 hormone-related genes were annotated as differentially expressed genes under Trend 1. In the correlation network analysis of Trend 1, the *MYB* gene family transcription factors demonstrated the notable connectivity. Specifically, *LlMYB44* (*TRINITY_DN21789_c0_g2*, *TRINITY_DN22732_c1_g1*, and *TRINITY_DN28694_c0_g1*) and *LlWRKY30* (*TRINITY_DN28933_c1_g1*) exhibited the highest connectivity, affecting the genes associated with the JA signal transduction pathway and plant hormone transport. For Trend 7, 100 TFs and 127 hormone-related genes were identified. The correlation network analysis for Trend 7 revealed that the most connected transcription factors were *LlMYB3R-1* (*TRINITY_DN28245_c0_g1*) and *LlE2FA* (*TRINITY_DN18686_c0_g1* and *TRINITY_DN18686_ c0_g2*), which primarily influenced the genes associated with plant hormone transport. In Trend 2, 21 TFs were annotated, along with 45 hormone-related DEGs. The network analysis for Trend 2 identified *LlWRKY2* (*TRINITY_DN28023_c0_g1*) as the most connected transcription factor, predominantly influencing the genes involved in the GA signal transduction pathway. Additionally, Trend 6 comprised 30 TFs among the differential genes, resulting in a total of 31 differential genes associated with hormones. The correlation network analysis for Trend 6 revealed that the most connected transcription factor was *LlDL* (*TRINITY_DN16235_c0_g1*) from the *YABBY* gene family, which was known for its role in lateral tissue formation and meristem function. Additionally, *LlPCF2* (*TRINITY_DN20505_c0_g7*) and *LlHSF4B* (*TRINITY_ DN19144_c0_g1*) indicated the high connectivity, primarily influencing the genes related to plant hormone transport. These genes could have a positive regulatory effect on the occurrence of bulbil. These findings further demonstrated the significance of plant hormones from the synthesis and transport to signal transduction in the development of *L. lancifolium* bulbils, emphasizing their pivotal roles in regulating bulbil occurrence.

Key genes involved in hormone pathways that affect the bulbil formation in *L. lancifolium*

Based on the botanical and anatomical observations, the *L. lancifolium* bulbil formation predominantly occurred in the upper half of the stem. Our focus was on two key periods, Ll_UN and Ll_DN, representing the stages with and without bulbils, respectively. The KEGG annotation revealed 78 DEGs related to auxin, 71 to jasmonate acid, 49 to gibberellin, and various numbers of cytokinin-, abscisic acid-, and salicylic acid-related DEGs (23, 22, and 9, respectively). Among the auxin-related DEGs, 49 encoded *SAUR* family proteins and 15 encoded Auxin Response Factors (*ARF*), most of which presented higher expression levels in Ll_UN stage. Among the jasmonate-related DEGs, 26 were encoded genes in the *JAZ* family and nine in the *bHLH* family. Additionally, 14 gibberellin-related DEGs encoded gibberellin 2-oxidase, and 11 encoded *DELLA* protein. Among the cytokinin-related differential genes, four encoded UDP-glycosyltransferases, displaying elevated expression levels during Ll_DN stage, whereas three others encoded the cytokinin dehydrogenase. The abscisic acid-related DEGs included six encoding abscisic acid receptors, mostly highly expressed in Ll_DN stage, and five encoding serine/threonine-protein kinase, predominantly expressed in Ll_UN stage. The salicylic acid-related DEGs included three encoding the transcription factor *TGA*, all of which exhibited higher expression during Ll_DN stage.

To provide a clearer understanding of the spatial distribution and alterations of each differential gene within the respective pathways, we integrated the pathway maps with heat maps (Fig. 3A and Fig.S4). Specifically, four pathways were focused including cytokinin, abscisic acid, gibberellin, and jasmonic acid synthesis. These DEGs were predominantly clustered within the gibberellin and jasmonate synthesis pathways and participated in the entire process. Notably, the DEGs within the plant hormone signal transduction pathway spanned various pathways, except the ethylene and brassinosteroid signal transduction pathways. Most DEGs in these two categories exhibited higher expression levels at Ll_DN stage.

We further refined these DEGs based on their *P*-values, resulting in a final selection of 46 DEGs (Table S6). Among these, 20 DEGs were associated with jasmonate, 16 with auxin, and three each with salicylic acid and abscisic acid. In addition, two DEGs were identified for both gibberellin and cytokinin, respectively. Finally, qRT-PCR analysis at Ll_UN and Ll_DN was conducted to validate the expression patterns of the candidate genes, leading to the identification of 11 candidate genes (Fig. 3B). These genes, namely *LlCCD4*, *LlTGA1*, *LlCYP74A2*, *LlIPT5*, *LlLOX2.1*, *LlGA2OX1*, *LlPYL4*, *LlTI-FY10A*, *LlARF6*, *LlbHLH41*, and *LlSAUR32*, were consistent with the transcriptome data. Notably, *LlCYP74A2*,

A

Cytokinin synthesis pathway

Abscisic acid synthesis pathway

Gibberelin synthesis pathway
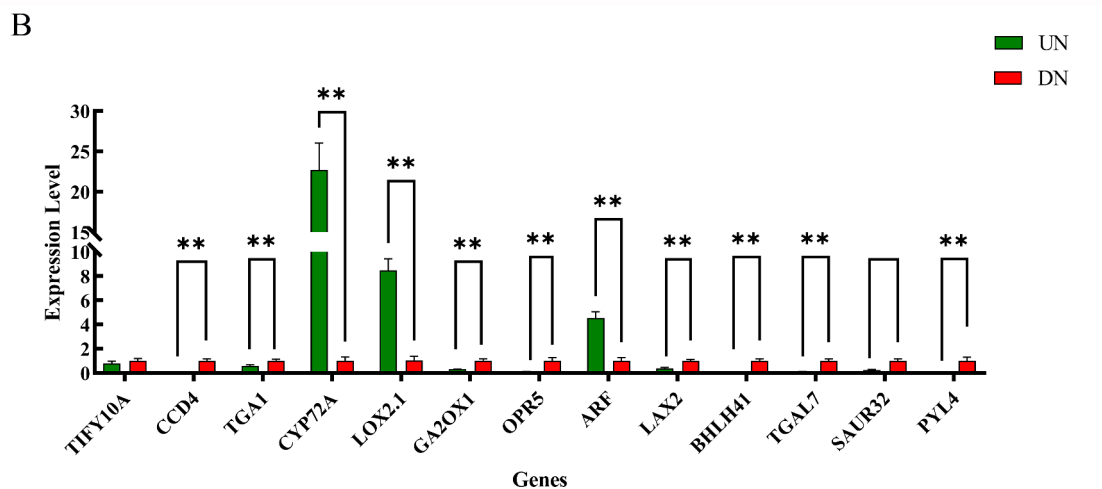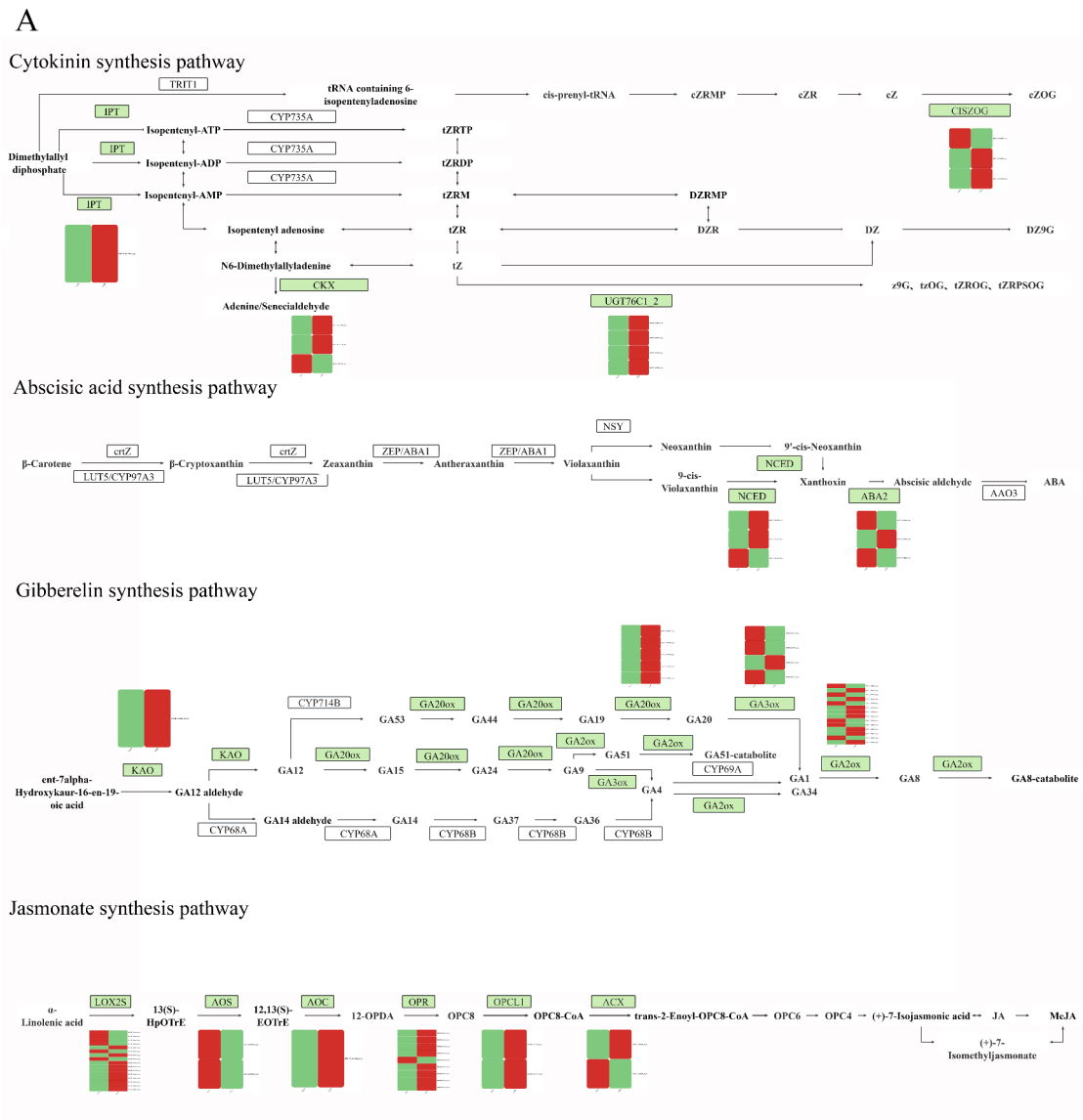
Jasmonate synthesis pathway

B

Fig. 3 Screened for differential gene and quantitative analysis. **(A)** Heat map of differential gene expression on the plant hormone synthesis pathway. **(B)** Quantitative results. Green rectangles represent the relative expression levels of the genes in LI_UN. Red rectangles represent the relative expression levels of the genes in LI_DN

Ma *et al. BMC Plant Biology*   (2024) 24:969

Page 8 of 17

LlLOX2.1, and *LlARF6* exhibited higher expression levels in Ll_UN than in Ll_DN, associated with the jasmonate synthesis and auxin signaling, respectively. Based on the aforementioned findings, we hypothesized that the regulation of *L. lancifolium* bulbils predominantly involved the jasmonate synthesis and signal transduction pathway, IAA signal transduction pathway, cytokinin synthesis pathway, and salicylate signal transduction pathway.

Key transcription factors (TF) regulating *L. lancifolium* bulbils

Given that axillary meristematic initiation was regulated by transcription factors, we identified the differential transcription factors from the selected genes in *L. lancifolium* transcriptome data. In Ll_DN vs. Ll_UN group, 311 significantly different TFs were identified. These transcription factors predominantly belonged to the *bHLH*, *ERF*, *MYB*, and *WRKY* gene families. The heatmap of these gene families was consistent with previous heatmap clustering (Fig. 4A) revealing that most of these differential transcription factors exhibited higher expression in Ll_DN stage than in Ll_UN stage. Moreover, all the differential TFs of the *WRKY* gene family indicated the higher expression in Ll_DN stage than in Ll_UN stage. To investigate the pivotal TFs involved in *L. lancifolium* bulbil occurrence, we conducted further screening based on expression levels. We identified differentially expressed TFs with a high correlation with previously screened genes by assessing their correlation. Subsequently, we associated these differential TFs with differential metabolites, using a threshold of 0.995. Ultimately, 27 TFs were identified (Table S7), comprising 11 from the *bHLH* gene family, 8 from the *WRKY* gene family, 4 from the *ERF* gene family, and 4 from the *MYB* gene family.

To gain a clearer understanding of the relationship between the 27 identified TFs, differential genes, and metabolites, we constructed a correlation network diagram (Fig. 4B). This revealed that all 27 TFs were highly correlated with differential jasmonate metabolites. *TRINITY_DN17758_c1_g2* (*LlbHLH30*), *TRINITY_DN19810_c0_g1* (*LlbHLH137*), *TRINITY_DN22416_c0_g1* (*LlbHLH144*), *TRINITY_DN22750_c0_g1* (LlbHLH106), and *TRINITY_DN26807_c0_g4* (*LlbHLH93*) were positively associated with jasmonate metabolite levels. They indicated the positive correlations with the genes involved in jasmonic acid synthesis pathway, such as *LlCYP74A2* and *LlLOX2.1*, and negative correlations with genes involved in the jasmonate signal transduction pathway, such as *LlbHLH41* and *LlTIFY10A*. This suggested that these five TFs positively regulated the jasmonate synthesis while inhibiting the jasmonate signal transduction, whereas other TFs exhibited the opposite pattern. Furthermore, these five transcription factors exhibited a positive correlation with differential

auxin-like metabolites, in contrast to other transcription factors. Conversely, only *TRINITY_DN18009_c1_g2* (*LlbHLH130*), *TRINITY_DN21011_c0_g2* (*LlbHLH144*), *TRINITY_DN25583_c0_g2* (*LlWRKY54*), and *TRINITY_DN29957_c0_g1* (*LlbHLH41*) were positively associated with differential salicylate metabolites. They displayed a strong positive correlation with *LlTGA1* genes involved in the salicylate signal transduction pathway. This suggested that these TFs could play a role in regulating the emergence of *L. lancifolium* bulbil sprouting by positively modulating salicylic acid signal transduction.

To validate the reliability of our previous findings, we conducted qRT-PCR analysis at Ll_UN and Ll_DN stages to confirm the expression patterns of the 11 candidate TFs, which were consistent with the transcriptome data (Fig. 4C). The majority of these transcription factors exhibited higher expression levels at Ll_DN stage. We hypothesized that this observation could contribute to the absence of bulbil formation in the lower part of the stem of *L. lancifolium*.

Effect of spraying exogenous hormone on the bulbil occurrence of *L. lancifolium*

In summary, we identified six key hormone categories using the screening process. To validate the efficiency of the hormones identified through metabolomic analysis, we conducted the exogenous spraying experiments. NPA (50, 100, and 150 mg/L), GA$_3$ (50, 100, and 150 mg/L), and MeJA (50, 100, and 150 μmol/L) were applied. Notably, the application of 50 mg/L NPA resulted in the most significant promotion of bulbil formation. The transparent bulges emerged on the 17th day after spraying and subsequently developed into white spherical bulges within 3 d. These bulges continued to expand and transition into green bulges around the 27th d after spraying (Fig. 5). Among the concentrations of spraying GA$_3$, 50 mg/L GA$_3$ proved to be the optimal concentration. The transparent bulges began to appear approximately 20 d after spraying and gradually expanded into the white bulges over the following week. For MeJA, the optimal concentration among the spray applications was 150 μmol/L, with bulge formation commencing approximately 27 d after spraying and continuing to expand thereafter. In contrast, the bulbil formation was not observed in the control group. These findings indicated that these hormones played a significant role of bulbil formation.

Through the integrated analysis of metabolome and transcriptome, we identified key DEGs and TFs, including the *LlPYL4* involved in the ABA signaling pathway, *LlbHLH137* and *LlbHLH93* in the JA synthesis, *LlTIFY10A* in the JA signal transduction, and *LlbHLH128* in the GA signal transduction. The core TFs, such as *LlbHLH41*, *LlWRKY6*, *LlWRKY24*, *LlbHLH63*, *LlMYB108*, and *LlRAX3*, were also identified. After the exogenous
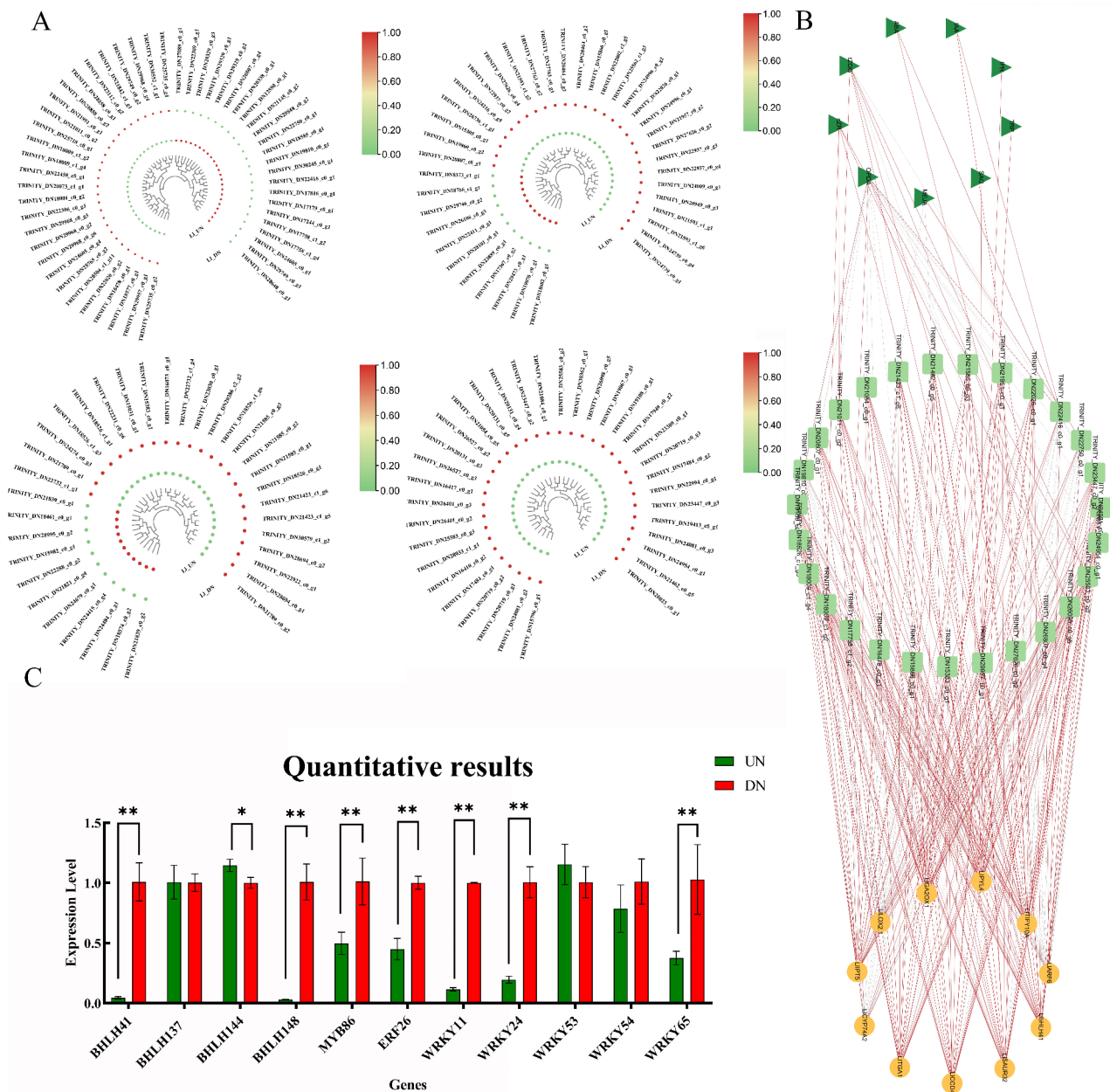
Fig. 4 Analysis of the screened-up transcription factors. (**A**) Heatmap of differential TFs. The *bHLH* gene family, *ERF* gene family, *MYB* gene family, and *WRKY* gene family, respectively. (**B**) Differential TFs with differential genes and differential metabolite correlation. Yellow circles represent the differential DEGs, green squares represent the differential TFs, green triangles represent the differential hormones. |rho|>0.995. (**C**) Quantitative results. Green rectangles represent the relative expression levels of the genes in Ll_UN. Red rectangles represent the relative expression levels of the genes in Ll_DN

spraying with 50 mg/L NPA, 50 mg/L GA$_3$, and 150 μmol/L MeJA, the emergence of *L. lancifolium* bulbils was significantly promoted. To investigate the direct relationship between these DEGs and TFs and their promoting hormones, as well as their role in bulbil occurrence, we conducted qRT-PCR analysis after spraying the three phytohormones that notably enhanced bulbil formation (Fig. 6). After spraying with NPA, GA$_3$, and MeJA, the *LlbHLH12*8, *LlTIFY10A*, *LlbHLH93*, and *LlMYB108*

exhibited consistent trends compared to the control group. This indicated that *LlbHLH128*, *LlTIFY10A*, and *LlMYB108* facilitated the bulbil initiation, whereas *LlbHLH93* exerted an inhibitory effect. Consequently, we identified *LlbHLH128*, *LlTIFY10A*, *LlbHLH93*, and *LlMYB108* as the pivotal genes involved in bulbil occurrence.
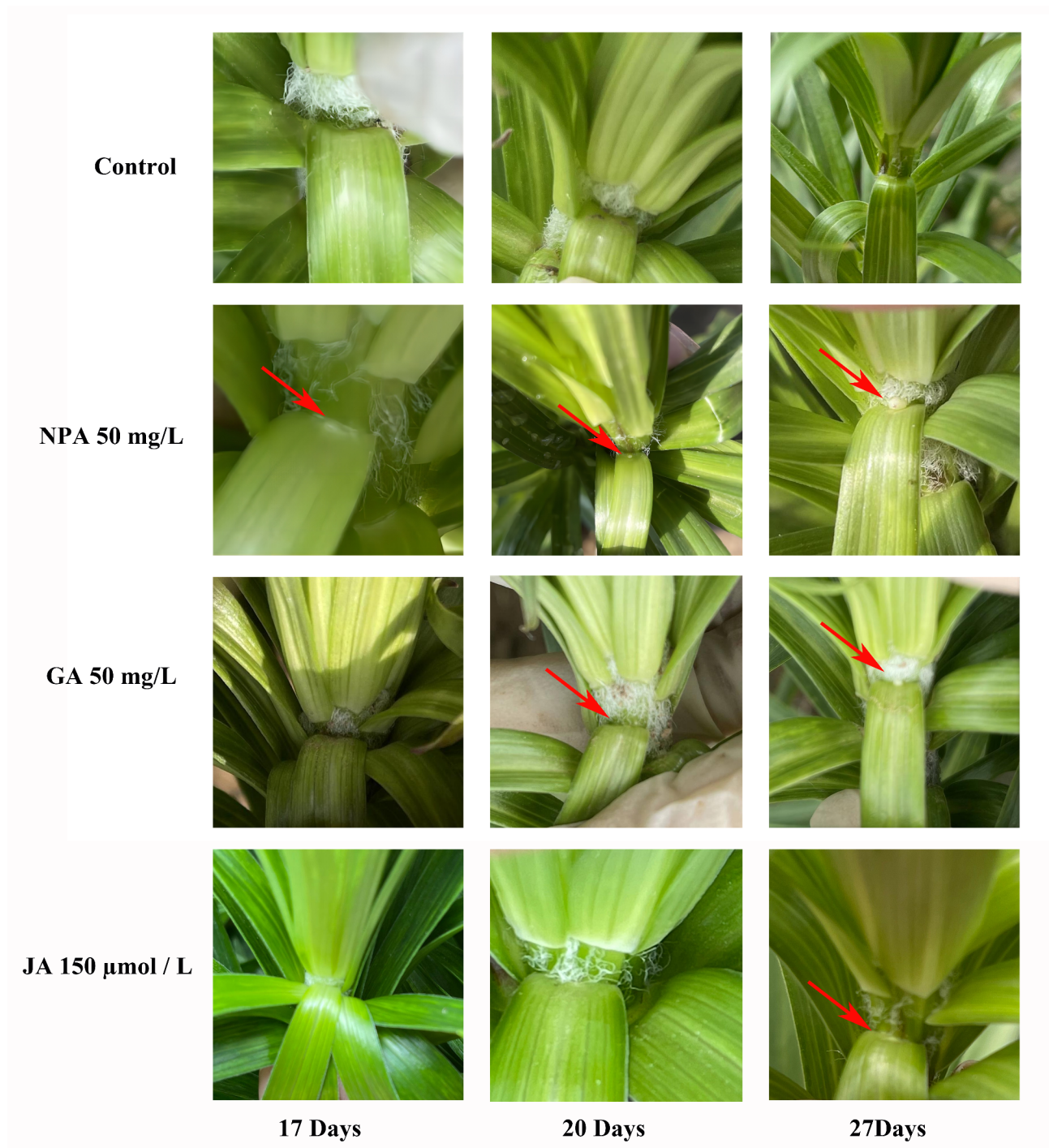
Fig. 5 The comparison of bulbil occurrence after spraying with 50 mg/LNPA, 50 mg/L GA$_3$ and 150 μ mol/L MeJA. Red arrows indicate the location of bulbil occurrence

Discussion

Multiple hormones act in concert for bulbil development

Previous metabolome assays have revealed slight variations in the types and levels of endogenous hormones across different developmental stages of *L. lancifolium* bulbils [3, 6]. Notably, during the initiation phase, there were significant changes in JA and IAA levels, with JA increasing and IAA decreasing. However, throughout the bulbil growth and development, certain hormones, such as DHZR and BR, remained unchanged. Additionally, mature bulbils can exhibit higher levels of IAA, GA$_3$, and
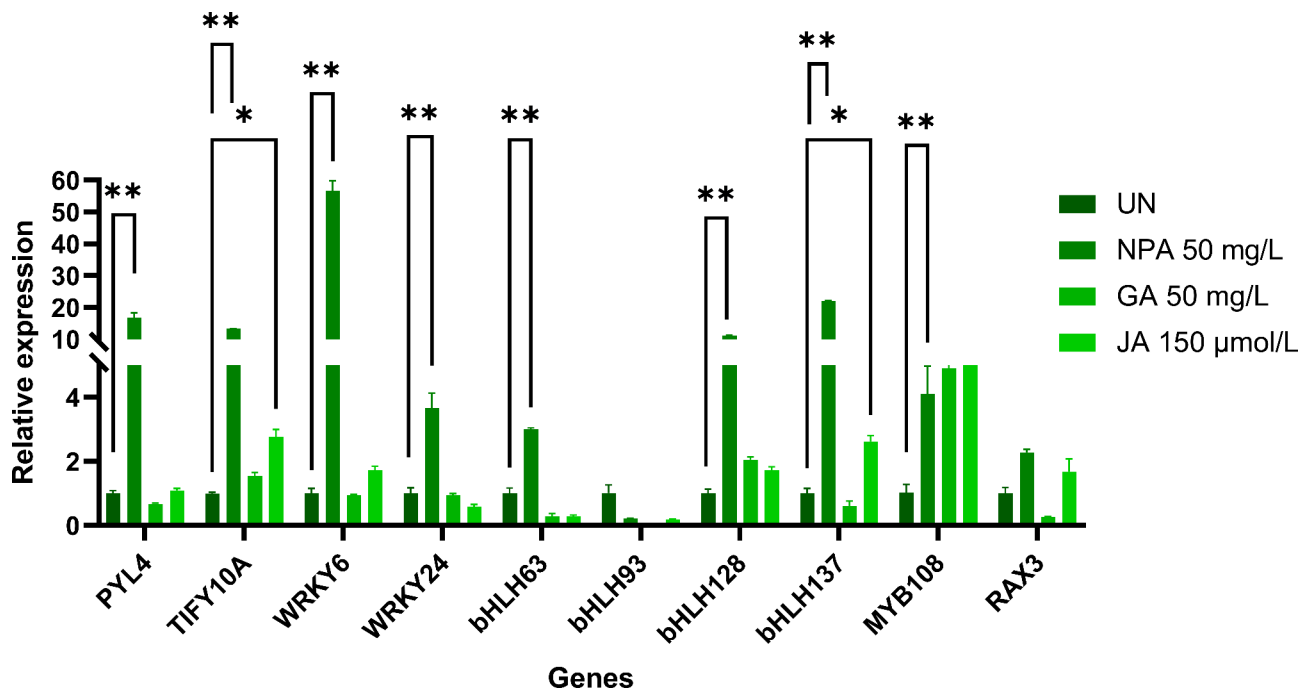
Fig. 6 The expression level of genes screened after spraying hormones

ABA than newborn bulbils, with ABA being more abundant in the upper axils than in the lower axils.

Molecular studies on lily bulbils, particularly those related to plant hormones, have been conducted. Research on *L. lancifolium* has primarily focused on the auxin- and cytokinin-related genes. For instance, Yang [2, 27] investigated the involvement of the auxin biosynthetic gene *YUCCA*, the catabolic gene *GH3*, the transport gene *PIN*, and response factors in bulbil development. Additionally, cytokinin has been shown to influence the occurrence of bulbils. He et al. [7, 8] proposed a model demonstrating how cytokinin promotes bulbil initiation and elucidated the molecular mechanism involving *WOX* genes and the cytokinin signaling pathway in regulating bulbil formation [9].

Through the systematic sampling and hormone determination, we discovered that the occurrence of *L. lancifolium* bulbils was caused by diverse hormones, namely ABA, IAA, GA, JA, CK, and SA. For the jasmonate-related hormones, excluding OPDA, their contents in stages without bulbils (Ll_UN and Ll_DN) were the lowest. However, as the bulbil growth progressed, the content gradually increased, peaking during the Ll_UE stage. OPDA was presumed to serve as a precursor for jasmonic acid synthesis. Hence, as bulbil growth advanced, its content gradually decreased. One reason for the presence or absence of bulbils on the upper and lower stems was the detection of CK-related hormones solely in the lower stem axilla but not in the upper three stages. Another reason could be the higher content of salicylic acid and

auxin in the Ll_DN stage than in other stages. These findings validated our results, indicating the involvement of multiple endogenous hormones in inducing bulbil development and growth.

TFs regulation of bulbil formation

L. lancifolium, as a triploid species, can naturally produce bulbils, which is very valuable to study bulbil occurrence in plants. The paraffin section revealed that the bulbils of *L. lancifolium* developed on the axils of the petiole base. These bulbils originated from the axillary meristem and differentiated into parenchyma, similar to lateral branches or tillers. There have been few researches on the bulbil formation compared to lateral branches and tillers. Yang et al.. hypothesized that *LlAGO1* may play a role in the lily bulbil formation, being expressed exclusively in the upper axils with bulbils [27]. *AGO1* was associated with the development of the lateral organs and axillary meristems [28]. To investigate whether the TFs identified as key regulators of bulbs were also linked to branching, we conducted the evolutionary tree analysis of branching-related genes with the selected genes in our experiment.

Some researchers have suggested that a subset of *R2R3-MYB* TFs primarily regulate the initiation of axillary tissue development [29]. In tomato, the *Blind* gene, which encodes a *MYB* TF, plays a significant role in regulating axillary meristem formation [31]. Our analysis revealed that the selected *MYB* gene family group *LlMYB108* contained *GmMYB181*, which was homologous to *AtMYB2*

(Fig. 7) [30–39]. *AtMYB2* was known to not only inhibit the AM formation but also impede its growth [37]. Our experimental findings further indicated that *LlMYB108* clustered with *AtMYB2* exhibited heightened expression at Ll_DN compared to the other three stages, suggesting its potential as a key transcription factor influencing the lower stem without bulbils.

The *bHLH* TFs serve as crucial regulatory elements in various developmental pathways [40]. *AtPIF4/PIF5* has been identified to stimulate IAA and ABA accumulation, as well as promote auxin and ABA signaling pathways, thereby influencing branching [43]. Additionally, *OsLAX2* plays a role in the initiation and maintenance of AM [48]. Within the screened *bHLH* gene family, *LlbHLH128* and *LlbHLH93* were grouped together *AtICE1* and *AtICE2* (Fig. 7) [29, 41–49]. *ICE2* is implicated in the regulation of axillary bud growth [41], and *JAZ1/TIFY10A* interacts with *ICE1* and *ICE2* [50]. Given its clustering with *LlbHLH128*, it was speculated that it could be directly involved in the bulbil occurrence. *LlbHLH93*, clustered with *AtICE1* and *AtICE2*, may potentially regulate the bulbil formation of *L. lancifolium* through interaction with *LlJAZ1/TIFY10A*, although further investigation could be needed to confirm it.

A hypothetic regulatory network affecting the bulbil formation of *L. lancifolium*

Moreover, it has been widely recognized that plant hormones interact extensively, forming a complex network that regulates plant growth and development. *JAZ1/TIFY10A* serves as a pivotal repressor of JA signaling, and its gene expression in *Arabidopsis* is induced not only by JA but also by early auxin response. Grunewald et al.. proposed that auxin-induced expression of *TIFY10A* contributed to an initial model of the auxin and JA signaling pathways [51].

Based on the aforementioned findings, we hypothesized that a similar model may also exist for *L. lancifolium*. We integrated this model with the pattern diagram presented above (Fig. 8), which revealed the intricate involvement of multiple plant hormones in bulbil induction. *LlbHLH93*, acting through *JAZ1/TIFY10A*, participated in the jasmonate signal transduction pathway and affected the occurrence of bulbil. However, *JAZ1/TIFY10A* not only affected the jasmonate signal transduction pathway but also engaged in the auxin signal transduction pathway, potentially indirectly affecting the bulbil formation by regulating *ARF* genes. Conversely, *LlbHLH128* and *LlMYB108* were speculated to directly regulate the bulbil formation. However, their roles differed, with one suppressing bulbil formation and the other promoting it.
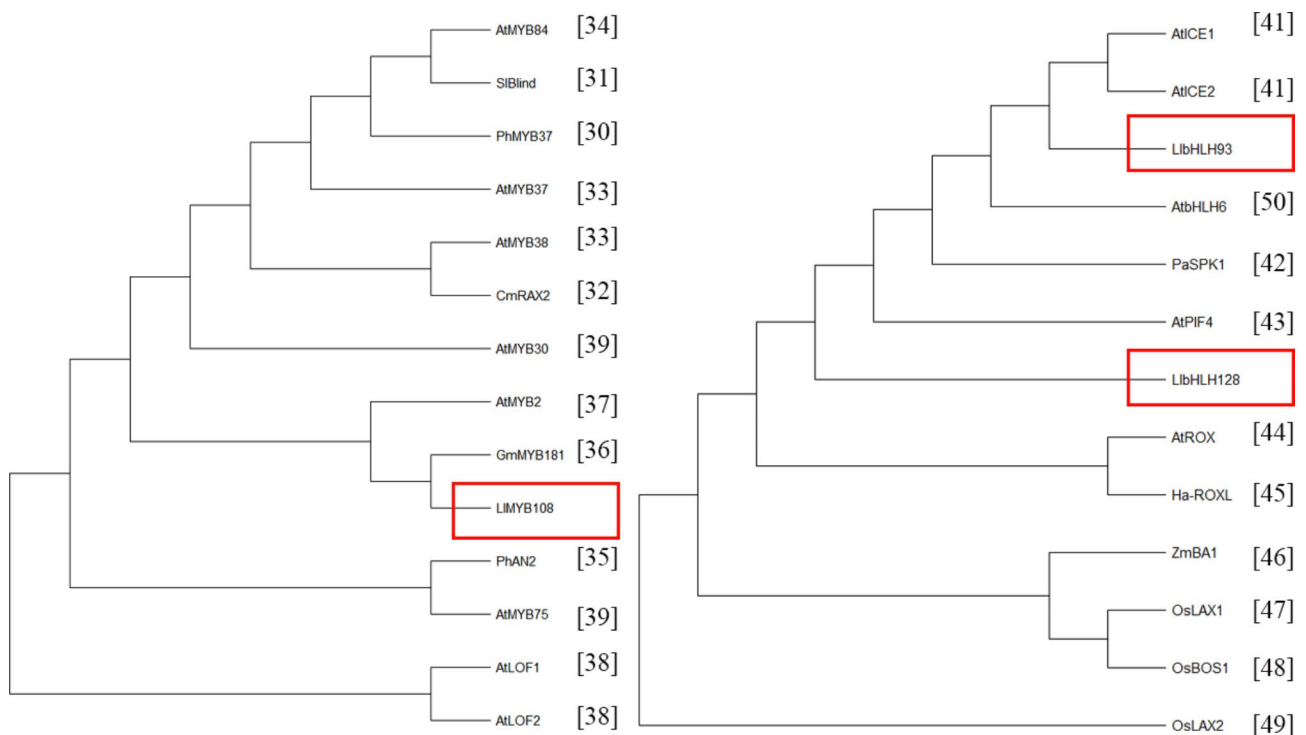

Fig. 7 Maximum likelihood (ML) tree of screened *MYB* genes and *bHLH* genes with known genes associated with branch in each family in different species
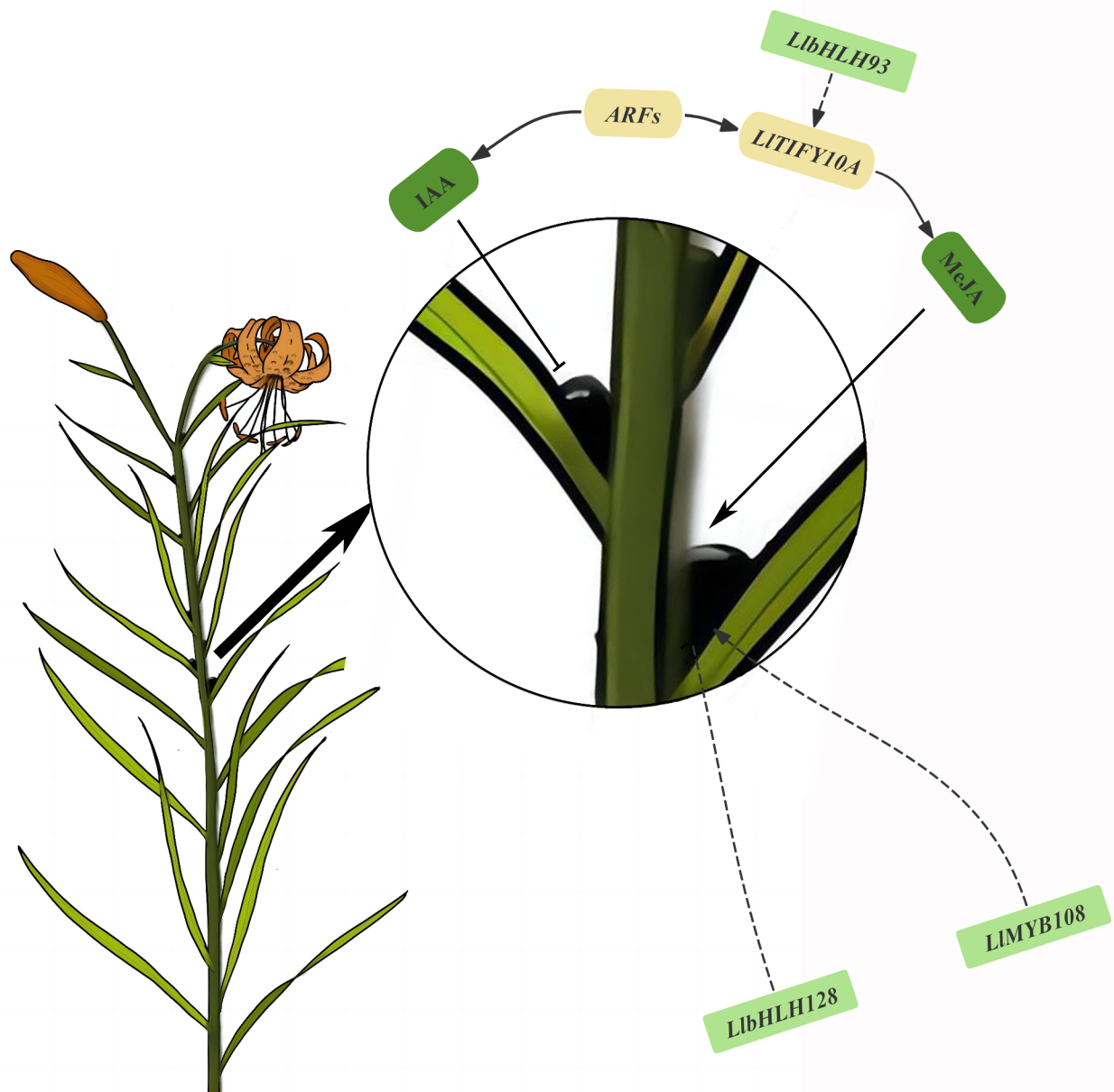
Fig. 8 A hypothetical regulatory network for the emergence of *L. lancifolium* bulbil. Arrows represent promotion, short horizontal lines indicate suppression, and dashed lines represent speculative relationship

The occurrence of *L. lancifolium* bulbils was a multifaceted process that could be regulated by numerous factors. Our aim was to identify the key factors influencing this process through our test results and existing studies, with the intention of offering guidance for future research.

Conclusions

Similar to plant branching, the regulation of *L. lancifolium* bulbil development was hypothesized to involve multiple factors, predominantly plant hormones, such as ABA, IAA, and JA. Through the transcriptome data screening and correlation analysis of differentially expressed hormones, the key TFs and structural genes were identified. The identified core TFs were categorized into *MYB*, *bHLH*, and *WRKY* gene families. The expression of these core genes was verified via qRT-PCR after spraying exogenous NPA, GA$_3$, and MeJA. Finally, *LlbHLH128*, *LlTIFY10A*, *LlbHLH93*, and *LlMYB108* were identified as the key genes associated with the bulbil formation. Building upon previous research, we aimed to elucidate the underlying mechanism, thereby contributing valuable insights into the intricate molecular network regulating bulbil formation.

Materials and methods

Plant materials

One hundred *L. lancifolium* bulbs were selected for cultivation in the open field in the National Lily Germplasm Repository at Shenyang Agricultural University, China. When the plants reached a height of 50 cm, the leaf axils were taken at a distance of 10 cm from the top of the stem. The growth state of the leaf axils at different stages was determined by paraffin section observation. The axils were dehydrated using various concentrations of ethanol, followed by the transparency with xylene at different gradients, and then embedded in paraffin. The paraffin-embedded tissue sections were sliced using a LEICA RM2255 microtome (Leica Biosystems, Wetzlar, Germany) at 8 μm thickness. These sections were subsequently stained with saffron and rapid green, and the digital images were captured using an Motic B410E camera system (Motic, Xiamen, China). This methodology aimed to identify the leaf axil stages that were crucial for studying the occurrence of *L. lancifolium* bulbils. Three periods of bulbil development on the upper stem: Ll_UN (Ll–*Lilium lancifolium*, no upper bulbils, U–upper, N–no), Ll_UT (transparent bulges in upper leaf axils, U–upper, T–transparent), and Ll_UE (white bulges emerging in upper leaf axils, U–upper, E–emerging), and one period of bulbil development on the lower stem: Ll_DN (no bulbils at 10 cm down from the bottom, D–down, N–no), were observed using the paraffin sections for transcriptome sequencing and metabolome determination (Fig. 1A-D, a-d). The axil samples were collected three replicates for each period. The samples were rapidly frozen in liquid nitrogen and stored at -80℃ for subsequent metabolome and transcriptome analyses.

Preparation and extraction of the metabolome samples

The frozen samples were ground into powder and dissolved in 1 mL of methanol/water/formic acid (15:4:1, v/v/v). To facilitate quantification, 10 μL of the internal standard mixed solution (100 ng/mL) was added to the extract as an internal standard (IS). The mixture was then extracted for 10 min, followed by centrifugation for 5 min at 4 °C and 12,000 rpm. The supernatant was transferred to clean plastic microtubes, evaporated to dryness, dissolved in 100 μL of 80% methanol, and filtered through a 0.22 μm membrane filter for subsequent LC-MS/MS analysis [52, 53].

Analysis of the hormone metabolome

The phytohormone levels of samples at various developmental stages were analyzed using the AB Sciex QTRAP 6500 LC-MS/MS platform by MetWare (http://www.metware.cn/). The standards of >99% purity were prepared in methanol (1 mg/mL). The Metware database (MWDB) was established using these standards for mass

spectrometry analysis. The data were acquired using Analyst 1.6.3 software (Sciex, Ontario, Canada), and all the metabolites were quantified using Multiplex 3.0.3 software (Sciex) [54–56].

The principal component analysis (PCA) facilitated an intuitive understanding of the variance and trends among all metabolites in *L. lancifolium* bulbils. Significantly regulated metabolites between groups were identified using t-test *P*-values and absolute log2fc (fold-change). R software was applied for the cluster analysis of metabolite content and to construct Wayne diagrams. The KEGG database (http://www.kegg.jp/kegg/compound/) was utilized to annotate different metabolites, followed by the classification and analysis of their metabolic pathway types (http://www.kegg.jp/kegg/pathway.html). The pathways with significantly regulated metabolites were subjected to the metabolite set enrichment analysis (MSEA), with the significance determined by the *P*-value of the hypergeometric test.

Effect of spraying exogenous hormone on bulbil emergence

The exogenous hormone treatments with NPA (50, 100, and 150 mg/L), GA$_3$ (50, 100, and 150 mg/L), and MeJA (50, 100, and 150 μmol/L) were administered by spraying every 7 d, starting from the 10 cm height stage and continuing until the visible flower bud stage. Distilled water was used as the control. Each treatment involved 60 independent plants and the emergence of bulbils was observed.

Total RNA extraction and library construction

Total RNA was extracted using TRIzol reagent (Invitrogen, Carlsbad, CA, USA), following the manufacturer's instructions. The quantity and purity of the RNA were assessed using a Bioanalyzer 2100 and RNA 1000 Nano LabChip Kit (Agilent, CA, USA), with a minimum RIN number>7.0. After purification, the cleaved RNA fragments were reverse-transcribed to generate 12 final cDNA libraries, including Ll_DN 1, Ll_DN 2, Ll_DN 3, Ll_UN 1, Ll_UN 2, Ll_UN 3, Ll_UT 1, Ll_UT 2, Ll_UT 3, Ll_UE 1, Ll_UE 2, and Ll_UE 3. The average insert size of the paired-end library prepared using the mRNASeq sample preparation kit (Illumina, San Diego, USA) was 300 bp (±50 bp). Paired-end sequencing was conducted on the Illumina Novaseq 6000 platform in the United States (LC Sciences), following the manufacturer's recommended protocol.

Data analysis with RNA-seq technology and differentially expressed unigene analysis

Initially, the internal processing involved the utilization of cutadapt and Perl scripts to eliminate reads containing adapter contamination, low-quality bases, and

undetermined bases [57]. Subsequently, the sequence quality validation was conducted using the FastQC software. De novo assembly of the transcriptome was performed using Trinity 2.4.0 [58]. All the assembled unigenes were aligned against various databases, including the non-redundant Gene Ontology (GO) (http://www.geneontology.org), Nr protein database (http://www.ncbi.nlm.nih.gov/), Kyoto Encyclopedia of Genes and Genomes (KEGG) (http://www.genome.jp/kegg/), SwissProt (http://www.expasy.ch/sprot/), and eggNOG (http://eggnogdb.embl.de/) databases using DIAMOND with an E-value threshold of <0.00001 [59].

The expression levels of unigenes were quantified using Salmon [60] by calculating TPM [61]. The differentially expressed unigenes were identified based on a log2 (fold change)>1 or log2 (fold change) < -1, with statistical significance determined using the R package edgeR [62].

The bioinformatic analysis was conducted using the OmicStudio tools available at https://www.omicstudio.cn/tool. The enrichment analysis was performed to identify the differential gene enrichment within the KEGG pathways. Additionally, a STEM (Short Time-series Expression Miner) was used for trend analysis of the differential genes.

Combined analysis of metabolomic and transcriptome groups

The differential genes and metabolites selected from both the metabolomic and transcriptomic groups were analyzed using the Pearson correlation analysis method. The correlation coefficient threshold≥0.8 and a correlation *P*-value<0.05 were set as the standards for this joint analysis, yielding the results. The correlation data between the differential genes and metabolites were generated using the OmicStudio tools available at https://www.omicstudio.cn/tool, followed by mapping with Cytoscape (Cytoscape_v3.9.1).

Gene expression analysis by qRT-PCR

With *EF1* as the internal reference gene (Gene Bank Accession Number: KJ543461) [63], according to the candidate gene sequence of unigenes obtained by splicing transcriptome, qRT-PCR primers were designed with Primer 3. Primers were sent to Bioengineering (Shanghai) Co., Ltd. for synthesis, as shown in Table S8.

The content of PCR products was detected by IQ5 (Bio-Rad, USA) PCR instrument with cDNA obtained by reverse transcription as template and SYBR Green as fluorescent dye. The $2^{-\Delta\Delta Ct}$ was used to calculate the relative expression difference. All the above data were plotted by GraphPad Prism 9, and variance analysis was performed by SPSS 17.0.

Supplementary Information

The online version contains supplementary material available at https://doi.org/10.1186/s12870-024-05654-9.

Supplementary Material 1

Supplementary Material 2

Supplementary Material 3

Supplementary Material 4

Supplementary Material 5

Supplementary Material 6

Supplementary Material 7

Supplementary Material 8

Supplementary Material 9

Supplementary Material 10

Supplementary Material 11

Supplementary Material 12

Supplementary Material 13

Author contributions
R. M. conceived the study and drafted the manuscript. Y. Z. and J. Z .analyzed the transcriptome data. Y. Z. analyzed the metabolome data. L. X. and J. L. revised the manuscript and provided guidance on the whole study. All authors contributed to the article and approved the submitted version.

Declarations

Ethics approval and consent to participate
Lilium lancifolium were collected from National Lily Germplasm Repository at Shenyang Agricultural University, China and were identified by professor Jiajun Lei. The methods involved in this study were carried out in compliance with local and national regulations.

Consent for publication
Not applicable.

Competing interests
The authors declare no competing interests.

References
1.   Jiang FX, Huang YX, Wang L, Zhou P, Sun DJ, Li X, Chen QB. Exploring the mystery of plant bulblet. Mol Plant Breed. 2017;15(1):346–52. https://doi.org/10.13271/j.mpb.015.000346.
2.   Yang PP, Xu LF, Xu H, Tang YC, He GR, Cao YW, Feng YY, Yuan SX, Ming J. Histological and transcriptomic analysis during bulbil formation in *Lilium lancifolium*. Front Plant Sci. 2017;8:1508. https://doi.org/10.3389/fpls.2017.01508.
3.   Fan JP, Bing W, Yan FX, Liu JS, Chen MX. Study on morphological characteristics and physiological changes of bulbils of *Lilium lancifolium*. J Northeast

Agricultural Univ. 2019;50(2):18–27. https://doi.org/10.19720/j.cnki.issn.1005-9369.2019.2.0003.

4. Bennett T, Leyser O. Something on the side: axillary meristems and plant development. Plant Mol Biol. 2006;60(6):843–54. https://doi.org/10.1007/s11103-005-2763-4.

5. Wang Q, Hasson A, Rossmann S, Theres K. Divide et impera: boundaries shape the plant body and initiate new meristems. New Phytol. 2016;209(2):485–98. https://doi.org/10.1111/nph.13641.

6. Luo R, Tian C, Xia LS, Chen HL, Du SS, Luo X. Cloning and expression analysis of *PteAUX1* gene related to bulblet development in *Pinellia ternata*. Molecular Plant Breeding: 2022; 1–19. https://kns.cnki.net/kcms/detail/46.1068.S.20210909.1656.026.html

7. He GR, Yang PP, Tang YC, Cao YW, Qi XY, Xu LF, Ming J. Mechanism of exogenous cytokinins inducing bulbil formation in *Lilium lancifolium* in vitro. Plant Cell Rep. 2020;39(1):861–72. https://doi.org/10.1007/s00299-020-02535-x.

8. He GR, Yang PP, Cao YW, Tang YC, Wang L, Song M, Wang J, Xu LF, Ming J. Cytokinin type-B response regulators promote bulbil initiation in *Lilium lancifolium*. Int J Mol Sci. 2021;22(7):3320. https://doi.org/10.3390/ijms22073320.

9. He GR, Cao YW, Wang J, Song M, Bi MM, Tang YH, Xu LF, Ming J, Yang PP. *WUSCHEL-related homeobox* genes cooperate with cytokinin to promote bulbil formation in *Lilium lancifolium*. Plant Physiol. 2022;190(1):387–402. https://doi.org/10.1093/plphys/kiac259.

10. Yang ML, Jiao YL. Regulation of axillary meristem initiation by transcription factors and plant hormones. Front Plant Sci. 2016;18(7):183. https://doi.org/10.3389/fpls.2016.00183.

11. Wang Y, Li J. Molecular basis of plant architecture. Annu Rev Plant Biol. 2008;59:253–79. https://doi.org/10.1146/annurev.arplant.59.032607.092902.

12. Gomez-Roldan V, Fermas S, Brewer PB, Puech-Pagès V, Dun EA, Pillot JP, Letisse F, Matusova R, Danoun S, Portais JC, Bouwmeester H, Bécard G, Beveridge CA, Rameau C, Rochange SF. Strigolactone inhibition of shoot branching. Nature. 2008;455:189–94. https://doi.org/10.1038/nature07271.

13. Janssen BJ, Drummond RS, Snowden KC. Regulation of axillary shoot development. Curr Opin Plant Biol. 2014;17:28–35. https://doi.org/10.1016/j.pbi.2013.11.004.

14. Yamaguchi S. Gibberellin metabolism and its regulation. Annu Rev Plant Biol. 2008;59:225–51. https://doi.org/10.1146/annurev.arplant.59.032607.092804.

15. Hong SY, Sun B, Straub D, Blaakmeer A, Mineri L, Koch J, Brinch-Pedersen H, Holme IB, Burow M, Lyngs Jørgensen HJ, Albà MM, Wenkel S. Heterologous microProtein expression identifies LITTLE NINJA, a dominant regulator of jasmonic acid signaling. Proc. Natl. Acad. Sci. 2020; 117, 26197–26205. https://doi.org/10.1073/pnas.2005198117

16. Waldie T, Leyser O. Cytokinin targets auxin transport to promote shoot branching. Plant Physiol. 2018;177(2):803–18. https://doi.org/10.1104/pp.17.01691.

17. Wang J, Yan DW, Yuan TT, Gao X, Lu YT. A gain-of-function mutation in I*AA8* alters *Arabidopsis* floral organ development by change of jasmonic acid level. Plant Mol Biol. 2013;82:71–83. https://doi.org/10.1007/s11103-013-0039-y.

18. Jiang FX, Wei PW, Wu S, Jiang XY, Shi JT, Chen QB. Transcriptional analysis of the pearl buds on the leaves of *Ornithogalum arabicum* L. Mol Plant Breed. 2017;15(2):519–31. https://doi.org/10.13271/j.mpb.015.000519.

19. Jiang FX, Huang YX, Zhou P, Sun XL, Song X, Chen QB. Cloning and functional analysis of *QtKN1* gene of *Ornithogalum arabicum* L. Mol Plant Breed. 2018;16(6):1777–83. https://doi.org/10.13271/j.mpb.016.001777.

20. Jiang FX, Wei KY, Sun XL, Song X, Wen HY, Chen QB. Cloning and characteristic analysis of *QtWOX8* gene of *Ornithogalum arabicum* L. Mol Plant Breed. 2018;16(14):4600–6. https://doi.org/10.13271/j.mpb.016.004600.

21. Jiang FX, Huang YX, Zhou P, Zhao J, Wen HY, Zhang L. Cloning and functional analysis of *OtDCAF8* gene of *Ornithogalum arabicum* L. Mol Plant Breed. 2019;17(21):7010–6. https://doi.org/10.13271/j.mpb.017.007010.

22. Rosin FM, Hart JK, Van Onckelen H, Hannapel DJ. Suppression of a vegetative *MADS* box gene of potato activates axillary meristem development. Plant Physiol. 2003;131(4):1613–22. https://doi.org/10.1104/pp.102.012500.

23. Jasinski S, Piazza P, Craft J, Hay A, Woolley L, Rieu I, Phillips A, Hedden P, Tsiantis M. *KNOX* action in *Arabidopsis* is mediated by coordinate regulation of cytokinin and gibberellin activities. Curr Biol. 2005;15(17):1560–5. https://doi.org/10.1016/j.cub.2005.07.023.

24. Abraham-Juárez MJ, Martínez-Hernández A, Leyva-González MA, Herrera-Estrella L, Simpson J. Class I *KNOX* genes are associated with organogenesis during bulbil formation in *Agave tequilana*. J Exp Bot. 2010;61(14):4055–67. https://doi.org/10.1093/jxb/erq215.

25. Delgado Sandoval S, del C, Abraham-Juárez MJ, Simpson J. *Agave tequilana MADS* genes show novel expression patterns in meristems, developing

26. Liu D, Luo R, Chen HL, Xia LS, Gao HX. Transcriptome and expression profile analysis revealed that *PEBP* gene family members were involved in the regulation of bulblet development of *Pinellia cordata*. J Guizhou Univ (Natural Sci Edition). 2018;35(2):48–53. https://doi.org/10.15958/j.cnki.gdxbzrb.2018.02.10.

27. Yang PP, Xu H, Xu LF, Tang YC, Ming J. Cloning and expression analysis of *LIAGO1* in *Lilium lancifolium*. Acta Horticulturae Sinica. 2018;45:784–94. https://doi.org/10.16420/jissn0513-353x2017-0601.

28. Bohmert K, Camus I, Bellini C, Bouchez D, Caboche M, Benning C. *AGO1* defines a novel locus of *Arabidopsis* controlling leaf development. EMBO J. 1998;17(1):170–80. https://doi.org/10.1093/emboj/17.1.170.

29. Yang F, Wang Q, Schmitz G, Müller D, Theres K. The *bHLH* protein *ROX* acts in concert with *RAX1* and *LAS* to modulate axillary meristem formation in *Arabidopsis*. Plant J. 2012;71(1):61–70. https://doi.org/10.1111/j.1365-313X.2012.04970.x.

30. Dong LL, Yang TY, Gao D, Wang T, Deng XY. *PhMYB37* promotes shoot branching in *Petunia*. Genes. 2022;13(11):2064. https://doi.org/10.3390/genes13112064.

31. Schmitz G, Tillmann E, Carriero F, Fiore C, Cellini F, Theres K. The tomato *blind* gene encodes a *MYB* transcription factor that controls the formation of lateral meristems. Proc Natl Acad Sci U S A. 2002;99(2):1064–9. https://doi.org/10.1073/pnas.022516199.

32. Song JJ, Chen YJ, Li X, Ma QQ, Liu QL, Pan YJ, Jiang BB. Cloning and functional verification of *CmRAX2* gene associated with chrysanthemum lateral branches development. Genes. 2022;27(5):779. https://doi.org/10.3390/genes13050779.

33. Müller D, Schmitz G, Theres K. Blind homologous R2R3 myb genes control the pattern of lateral meristem initiation in *Arabidopsis*. Plant Cell. 2006;18(3):586–97. https://doi.org/10.1105/tpc.105.038745.

34. Guo DS, Zhang JZ, Wang XL, Han X, Wei BY, Wang JQ, Li BX, Yu H, Huang QP, Gu HY, Qu LJ, Qin GJ, The. *WRKY* transcription factor *WRKY71/EXB1* controls shoot branching by transcriptionally regulating *RAX* genes in *Arabidopsis*. Plant Cell. 2015;27(11):3112-27. https://doi.org/10.1105/tpc.15.00829

35. Li G, Serek M, Gehl C. Physiological changes besides the enhancement of pigmentation in Petunia hybrida caused by overexpression of PhAN2, an R2R3-MYB transcription factor. Plant Cell Rep. 2023;42(3):609–27. https://doi.org/10.1007/s00299-023-02983-1.

36. Yang H, Xue Q, Zhang ZZ, Du JY, Yu DY, Huang F. *GmMYB181*, a soybean *R2R3-MYB* protein, increases branch number in transgenic *Arabidopsis*. Front Plant Sci. 2018;9:1027. https://doi.org/10.3389/fpls.2018.01027.

37. Jia TQ, Zhang KD, Li F, Huang YF, Fan MM, Huang T. The *AtMYB2* inhibits the formation of axillary meristem in *Arabidopsis* by repressing *RAX1* gene under environmental stresses. Plant Cell Rep. 2020;39(12):1755–65. https://doi.org/10.1007/s00299-020-02602-3.

38. Lee DK, Geisler M, Springer PS. *LATERAL ORGAN FUSION1* and *LATERAL ORGAN FUSION2* function in lateral organ separation and axillary meristem formation in *Arabidopsis*. Development. 2009;136(14):2423–32. https://doi.org/10.1242/dev.031971.

39. Zhou HP, He JX, Zhang YY, Zhao HY, Sun X, Chen X, Liu XR, Zheng Y, Lin HH. *RHA2b*-mediated *MYB30* degradation facilitates *MYB75*-regulated, sucrose-induced anthocyanin biosynthesis in *Arabidopsis* seedlings. Plant Commun. 2024;5(3):100744. https://doi.org/10.1016/j.xplc.2023.100744.

40. Heim MA, Jakoby M, Werber M, Martin C, Weisshaar B, Bailey PC. The basic helix-loop-helix transcription factor family in plants: a genome-wide study of protein structure and functional diversity. Mol Biol Evol. 2003;20:735–47. https://doi.org/10.1093/molbev/msg088.

41. Kurbidaeva A, Ezhova T, Novokreshchenova M. Arabidopsis thaliana ICE2 gene: phylogeny, structural evolution and functional diversification from ICE1. Plant Sci. 2014;229:10–22. https://doi.org/10.1016/j.plantsci.2014.08.011.

42. Lin YJ, Li MJ, Hsing HC, Chen TK, Yang TT, Ko SS. *activatorivator 1*, encoding a *bHLH*, mediates axillary bud development and spike initiation in *PhalaenAphroditerodite*. Int J Mol Sci. 2019;30(21):5406. https://doi.org/10.3390/ijms20215406.

43. Holalu SV, Reddy SK, Blackman BK, Finlayson SA. Phytochrome interacting factors 4 and 5 regulate axillary branching via bud abscisic acid and stem auxin signalling. Plant Cell Environ. 2020;43(9):2224–38. https://doi.org/10.1111/pce.13824.

44. Basile A, Fambrini M, Tani C, Shukla V, Licausi F, Pugliesi C. The *Ha-ROXL* gene is required for initiation of axillary and floral meristems in sunflower. Genesis. 2019;57(9):e23307. https://doi.org/10.1002/dvg.23307.

bulbils and floral organs. Sex Plant Reprod. 2012;25(1):11–26. https://doi.org/10.1007/s00497-011-0176-x.

45. Yao H, Skirpan A, Wardell B, Matthes MS, Best NB, McCubbin T, Durbak A, Smith T, Malcomber S, McSteen P. The barren *stalk2* gene is required for axillary meristem development in maize. Mol Plant. 2019;12(3):374–89. https://doi.org/10.1016/j.molp.2018.12.024.

46. Mach J. Rice axillary meristem formation requires directional movement of *LAX PANICLE1* protein. Plant Cell. 2009;21(4):1027. https://doi.org/10.1105/tpc.109.210410.

47. Lv YP, Zhang XF, Hu YJ, Liu S, Yin YB, Wang XX. *BOS1* is a basic helix-loop-helix transcription factor involved in regulating panicle development in rice. Front Plant Sci. 2023;14:1162828. https://doi.org/10.3389/fpls.2023.1162828.

48. Tabuchi H, Zhang Y, Hattori S, Omae M, Shimizu-Sato S, Oikawa T, Qian Q, Nishimura M, Kitano H, Xie H, Fang X, Yoshida H, Kyozuka J, Chen F, Sato Y. *LAX PANICLE2* of rice encodes a novel nuclear protein and regulates the formation of axillary meristems. Plant Cell. 2011;23(9):3276–87. https://doi.org/10.1105/tpc.111.088765.

49. He KR, Du JC, Han X, Li HQ, Kui MY, Zhang JP, Huang ZC, Fu QT, Jiang YJ, Hu YR. *PHOSPHATE STARVATION RESPONSE1* (*PHR1*) interacts with *JASMONATE ZIM-DOMAIN (JAZ)* and *MYC2* to modulate phosphate deficiency-induced jasmonate signaling in *Arabidopsis*. Plant Cell. 2023;35(6):2132–56. https://doi.org/10.1093/plcell/koad057.

50. Hu YR, Jiang LQ, Wang F, Yu DQ. Jasmonate regulates the *INDUCER OF CBF EXPRESSION-C-REPEAT BINDING FACTOR/DRE BINDING FACTOR1* cascade and freezing tolerance in *Arabidopsis*. Plant Cell. 2013;25(8):2907–24. https://doi.org/10.1105/tpc.113.112631.

51. Grunewald W, Vanholme B, Pauwels L, Plovie E, Inzé D, Gheysen G, Goossens A. Expression of the *Arabidopsis* jasmonate signalling repressor *JAZ1/TIFY10A* is stimulated by auxin. EMBO Rep. 2009;10(8):923–8. https://doi.org/10.1038/embor.2009.103.

52. Floková K, Tarkowská D, Miersch O, Strnad M, Wasternack C, Novák O. UHPLC-MS/MS based target profiling of stress-induced phytohormones. Phytochemistry. 2014;105:147–57. https://doi.org/10.1016/j.phytochem.2014.05.015.

53. Li Y, Zhou CX, Yan XJ, Zhang JR, Xu JL. Simultaneous analysis of ten phytohormones in *Sargassum Horneri* by high-performance liquid chromatography with electrospray ionization tandem mass spectrometry. J Sep Sci. 2016;39(10):1804–13. https://doi.org/10.1002/jssc.201501239.

54. Pan XQ, Welti R, Wang XM. Quantitative analysis of major plant hormones in crude plant extracts by high-performance liquid chromatography-mass spectrometry. Nat Protoc. 2010;5(6):986–92. https://doi.org/10.1038/nprot.2010.37.

55. Cui KY, Lin YY, Zhou XY, Li SC, Liu H, Zeng F, Zhu F, Ouyang GF, Zeng ZX. Comparison of sample pretreatment methods for the determination of multiple phytohormones in plant samples by liquid chromatography-electrospray ionization-tandem mass spectrometry. Microchem J. 2015;121:25–31. https://doi.org/10.1016/j.microc.2015.02.004.

56. Šimura J, Antoniadi I, Široká J, Tarkowská D, Strnad M, Ljung K, Novák O. Plant hormonomics: multiple phytohormone profiling by targeted metabolomics. Plant Physiol. 2018;177(2):476–89. https://doi.org/10.1104/pp.18.00293.

57. Martin M. Cutadapt removes adapter sequences from high-throughput sequencing reads EMBnet. Journal. 2011;10–2. https://doi.org/10.14806/EJ.17.1.200. ISSN 2226–6089.

58. Grabherr MG, Haas BJ, Yassour M, Levin JZ, Thompson DA, Amit I, Adiconis X, Fan L, Raychowdhury R, Zeng Q, Chen Z, Mauceli E, Hacohen N, Gnirke A, Rhind N, di Palma F, Birren BW, Nusbaum C, Lindblad-Toh K, Friedman N, Regev A. Full-length transcriptome assembly from RNA-Seq data without a reference genome. Nat Biotechnol. 2011;29(7):644–52. https://doi.org/10.1038/nbt.1883.

59. Buchfink B, Xie C, Huson DH. Fast and sensitive protein alignment using DIAMOND. Nat Methods. 2015;12(1):59–60. https://doi.org/10.1038/nmeth.3176.

60. Patro R, Duggal G, Love MI, Irizarry RA, Kingsford C. Salmon provides fast and bias-aware quantification of transcript expression. Nat Methods. 2017;14(4):417–9. https://doi.org/10.1038/nmeth.4197.

61. Mortazavi A, Williams BA, McCue K, Schaeffer L, Wold B. Mapping and quantifying mammalian transcriptomes by RNA-Seq. Nat Methods. 2008;5(7):621–8. https://doi.org/10.1038/nmeth.1226.

62. Robinson MD, McCarthy DJ, Smyth GK. Bioinformatics. 2010;26(1):139–40. https://doi.org/10.1093/bioinformatics/btp616. edgeR: a Bioconductor package for differential expression analysis of digital gene expression data.

63. Chen MM, Zhang RJ, Cha Q, Yang LY, Li Xin, Yin LQ, Zhang YC. Induction and development of lily somatic embryos and screening of real-time quantitative PCR internal reference genes in different tissues. Mol Plant Breed. 2018;16(15):4982–90. https://doi.org/10.13271/j.mpb.016.004982.

Publisher's note